Australian Government
Bureau of Rural Sciences

Identifying acid sulfate soil hotspots from airborne gamma-radiometric data and GIS analysis

P.N Bierwirth and R.S Brodie

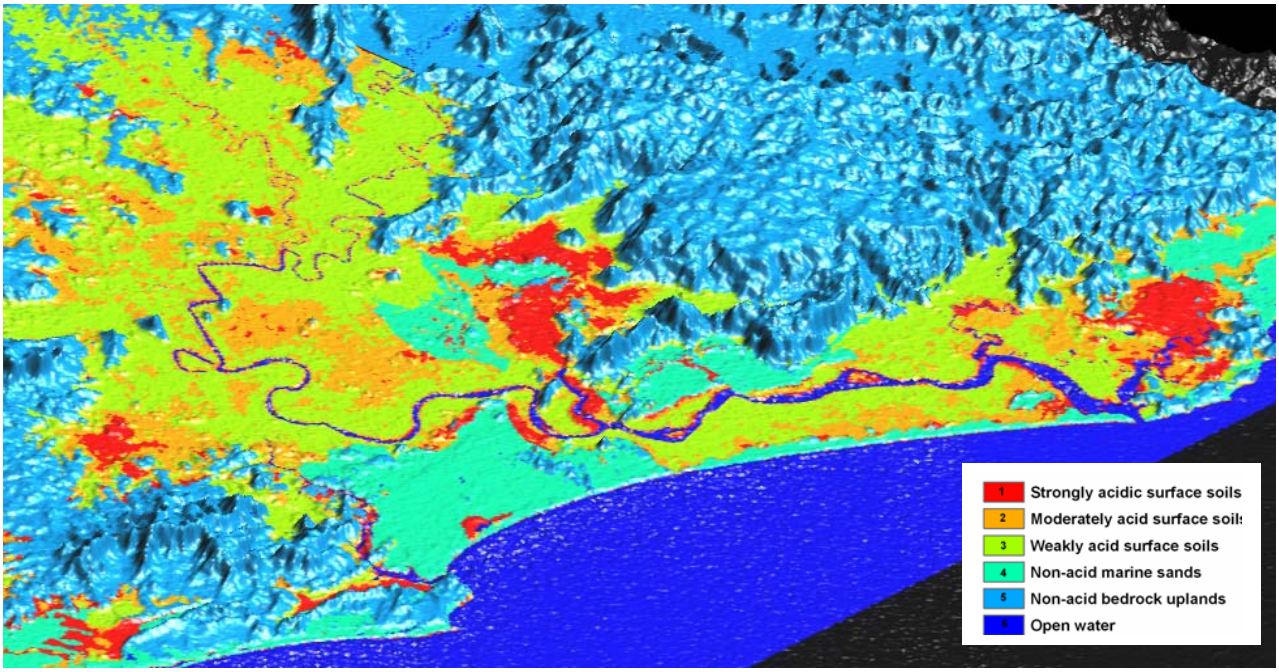

Postal address:
Bureau of Rural Sciences
GPO Box 858
Canberra ACT 2601

Email: salesbrs@brs.gov.au

Internet: http://www.brs.gov.au

Copies available from:
http://www.brs.gov.au/publications

Cover Figure: Three-dimensional perspective of the predicted distribution of acid areas within the Lower Richmond floodplain, northern New South Wales. These areas have been defined by GIS modelling of gamma-ray remote sensing data.

Contents

Figures

Tables

Executive Summary

Acid sulfate soils are estuarine pyritic sediments found along the Australian coastal zone. When maintained under waterlogged and reduced conditions these sediments are stable. However if these sediments are disturbed or dewatered, the sulfides can oxidise, generating sulfuric acid. This acidification is a significant land and water management issue, being responsible for denuded acid scalds, lost agricultural productivity, fish and oyster kills, poor water quality, altered ecology and infrastructure damage.

Mapping the distribution of acid sulfate soils is an important precursor for appropriate management. To this end, gamma-radiometric surveys are an important tool for mapping the properties of soils and their parent geological material. These surveys produce image data of the concentration of gamma-ray emitting elements, principally potassium (K), thorium (Th) and uranium (U). A regional airborne radiometric survey of part of the coastal zone of northern New South Wales was assessed to test the usefulness of these datasets in identifying acid sulfate soil areas.

The thorium concentration imagery shows the greatest potential for mapping areas of active acidification. Independent mapping of high acid risk areas could be correlated with areas of very low thorium concentration. This is because the solubility of thorium is greatly enhanced in the acidic, sulfate- and organic-rich groundwaters found in these areas. On this basis, it is inferred that mobilisation and flushing of thorium from the soil profile can occur in areas of long-term acidification. On-ground measurements using a portable spectrometer confirmed this relationship between actual acid sulfate soils and thorium depletion. Similar depletion occurred in these environments for uranium, however the uranium concentration imagery has greater spatial noise. Hence, uranium also appears to have the potential to map soil acidification, but more so using ground-based surveys that have greater resolution than airborne surveys.

However, other landscape units in the coastal zone also have a low-thorium signature, mainly surface water bodies, quartzose marine sands and basalt/sandstone outcrops. Masking of these areas was largely successful using a digital elevation model, satellite solar reflectance and available geological mapping. Soil moisture can also attenuate the thorium signal and needs to be considered in the data analysis. Due to the effects of water, it is recommended that any gamma radiometric surveys in the coastal zone be undertaken during the dry season.

This work highlights the potential for using airborne radiometric surveys to target the worst areas of intense acidification that require further investigation and to prioritise investment of on-ground works. The methodology is generic as it is based on the mobilisation of thorium in an acid environment, so should be transferable to other coastal catchments. This is significant considering that there is an estimated 13.5 million hectares of acid sulfate soils globally, with 1 million hectares in Australia (White *et al*, 1995). Gamma ray data from airborne surveys is already available in the public domain for parts of the Australian coastal zone. This is a new application of these surveys and is complementary to the existing methods of mapping acid sulfate soils such as airphoto interpretation and soil sampling. The method can provide new information about coastal geomorphology as well as acidification in the near-surface. It is cost-effective on a per-hectare basis and rapid. It also has the advantages that other geophysical techniques (such as magnetics or electromagnetics) can also be incorporated into any proposed airborne survey and that the radiometrics data can be used for other purposes (such as mapping other soil properties and types).

1. Introduction

In the coastal zone of Australia, the impacts of disturbing acid sulfate soils are a significant land and water management issue. Acid sulfate soils (ASS) are based on sediments deposited under estuarine conditions that contain the iron sulfide pyrite. When maintained in a waterlogged and reduced condition, these sediments are stable and are termed potential acid sulfate soils (PASS). However, activities such as road construction, drainage, cropping, urban development or mining can expose these sediments to air. This allows oxidation of the pyrite which is a chemical reaction that generates sulfuric acid. The soil profile can acidify (pH < 4) to form actual acid sulfate soils (AASS). Severe soil acidification can lead to the development of denuded acid scalds. These areas are associated with greatly reduced agricultural productivity or degraded ecological values. Acid water can flocculate clays, resulting in soil fabric deterioration such as soil shrinkage and ground subsidence (White *et al*, 1997).

Following rainfall, the store of acid can migrate into drains and be exported to wetlands and estuaries. The acid water can dissolve iron, aluminium and other metals to levels that are toxic to aquatic life, resulting in fish kills. Increased dissolution of silica can also initiate algal blooms (Tulau, 1999a). Secondary precipitates of iron and aluminium can smother benthos and aquatic plants. Deoxygenated water generated by the secondary oxidation of iron can also cause fish kills. The chronic effects on aquatic life also include fish disease outbreaks, reduced food resources, limitations on the migration potential for fish, reduced fish recruitment and altered ecology such as weed invasion by acid-tolerant plants (Sammut *et al*, 1996). The acid water can also cause infrastructure damage due to the corrosion of concrete and metal.

Mapping the distribution of acid sulfate soils is an important precursor for appropriate management. Mapping initiatives in New South Wales (Naylor *et al*, 1998) and Queensland (Powell & Ahern, 1999; Hey, 1999) have been based on topographic and geomorphic criteria, involving airphoto interpretation followed by field checking and soil sampling. Published generic soil maps using the Australian Soil Classification (Isbell, 1996), geological maps showing Holocene estuarine deposits, as well as standard topographic maps have also proven to be useful in identifying acid sulfate soils (Hey, 1999).

Ongoing development of satellite or aircraft-based remote sensing platforms now gives the opportunity to supplement or validate this conventional approach to mapping. In this paper, we focus on the use of one such technology, that of airborne radiometrics, to help target acid sulfate soil hotspots at the catchment reconnaissance level.

2. Airborne Radiometric Survey

2.1 Methodology

Airborne radiometric surveys measure the natural radiation in the shallow soil/rock profile and are used as a geological mapping tool, particularly in the mineral exploration industry. The technique is also used by soil scientists and geomorphologists to map the distribution and properties of soil or landscape units.

Radiometrics is also called gamma-ray spectrometry, as it is based on the measurement of gamma rays emitted with the decay of naturally occurring radioactive elements, principally from potassium (K), thorium (Th) and uranium (U). A spectrometer is used to count the number of gamma rays across multiple bands within the energy spectrum. Peaks in particular bands can be attributed to each of the three radioactive elements considered. In this way, the gamma ray signature can be used to measure the abundances of potassium, thorium and uranium in the soil profile. Since gamma-rays are strongly attenuated, most of the radiation emanates from shallow ground depth, with 90% of measured gamma-rays received from the top 30-45 cm for a dry overburden of density 1.5 g/cm^3 (Grasty, 1976).

Airborne radiometric surveys use either helicopters or fixed-wing aircraft, depending on the terrain. The survey is undertaken along flightlines in a fixed direction (eg east-west) that are separated by a fixed distance (eg 200 metres). Along each flightline, a reading is taken at a fixed time interval (eg 1 second), with the aircraft speed defining the sample distance along the ground (eg 30 – 80m). The data is interpolated between flight lines, resulting in grids of mean ground-level abundances of potassium, thorium and uranium.

These gridded datasets can provide detailed information about the characteristics of the soil and its parent geological material, including surface texture, weathering, leaching, soil depth, moisture and clay mineralogy (Bierwirth, 1997). The technique is particularly useful as the imagery is not significantly masked by atmospheric or vegetation effects, which is an issue for other remote sensing platforms such as Landsat TM when investigating soil properties. It has been estimated that dense vegetation will reduce the measured element concentrations by only about 15% (Aspin & Bierwirth, 1997). On-ground radiometric surveys using portable spectrometers are particularly valuable in validating airborne surveys, checking anomalies or to provide more detailed soil mapping.

2.2 Application to Acid Sulfate Soil Mapping

In 1996, the then Australian Geological Survey Organisation (AGSO) flew a regional airborne geophysical survey over the lower reaches of the Clarence and Richmond catchments (as well as offshore areas) of northern New South Wales (Figure 1). The survey spanned two time periods, from 5 to 13 March and from 11 August to 28 September. The survey combined the collection of gamma-ray spectrometric data with magnetic and digital elevation model (DEM) data, with the three-fold objective of discriminating coastal environments; targeting areas of coastal land degradation; and examining the structure of the continental shelf (Mitchell & Minty, 1998).

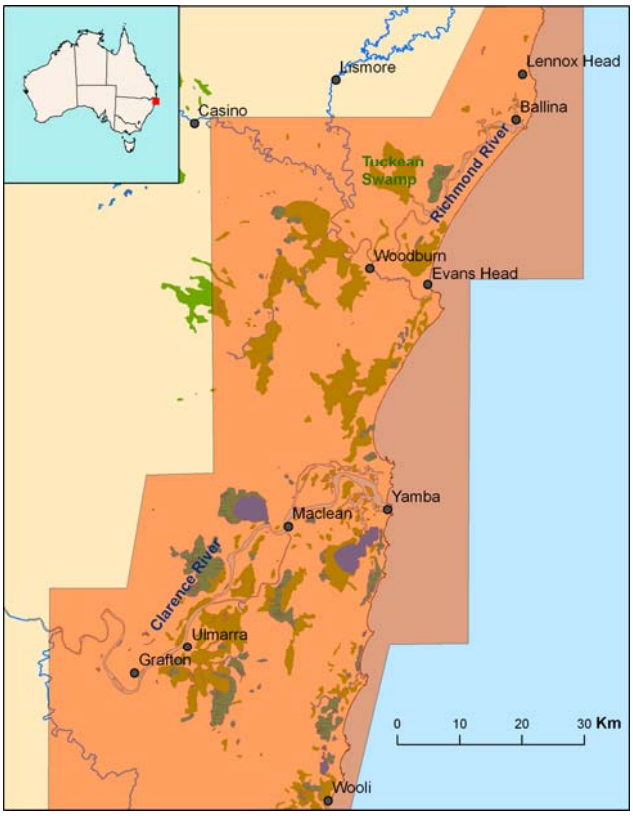

Figure 1: Location of Clarence Richmond airborne geophysical survey and Tuckean Swamp case study area

The survey is an unprecedented opportunity for applying gamma-ray spectrometry to the mapping of acid sulfate soils. In this regard, initial interpretation focussed on the potassium concentration imagery generated from the gamma-ray survey in combination with iron-oxide mapping using Landsat TM (Bierwirth & Graham, 1998). In lowland areas, levee floodplain deposits could be discriminated on the basis of high potassium levels, reflecting mineralogy relating to silt particles. Although not a direct indicator of acid sulfate soils, this has the potential to screen areas with levee floodplain cover, which could be areas of relatively low risk in terms of acidification.

Although potassium levels can relate to pH in some landscapes (Bierwirth, 1997), this element is highly mobile in a range of conditions and often indicates the degree of weathering in a landscape. The other components of the radiometrics, namely the thorium and uranium concentrations, have the potential to more directly map acid sulfate soils. This is largely based on the effect that acidification has on the solubility and subsequent mobilisation of these elements.

Thorium (Th) is typically found in heavy minerals such as zircon and monazite that are highly resistant to weathering, so has long been considered insoluble in natural waters. Thorium is also sorbed onto clays and soil colloids, so the initial expectation would be that the clay-rich sediments of estuarine and backswamp environments would have average (or higher) thorium concentrations. However, in acid conditions (pH < 3), hydrous ThO_2 is quite soluble and the Th^{4+} cation is stable (Katz et al, 1986), refer Figure 2. Studies have shown that thorium forms strong complexes with sulfate, fluoride, phosphate, hydroxide and organic anions, particularly in low pH conditions (Langmuir & Herman, 1980). The formation of these complexes greatly enhances the solubility of thorium (Figure 2). For example, dissolution increases by three orders of magnitude at pH of 3 in the presence of 100 mg/L total sulfate. Likewise small concentrations of organic ligands have the same effect. Langmuir and Herman (1980) also cite the example that 1mg/L of total oxalate increases thorium solubility by 10^7 times at pH 4. These strong organic complexes also inhibit the adsorption of thorium onto clays and other

colloidal material. As well, with decreased crystallinity of the host solid, the dissolution of thorium will occur at higher pH (Hummel, 2005).

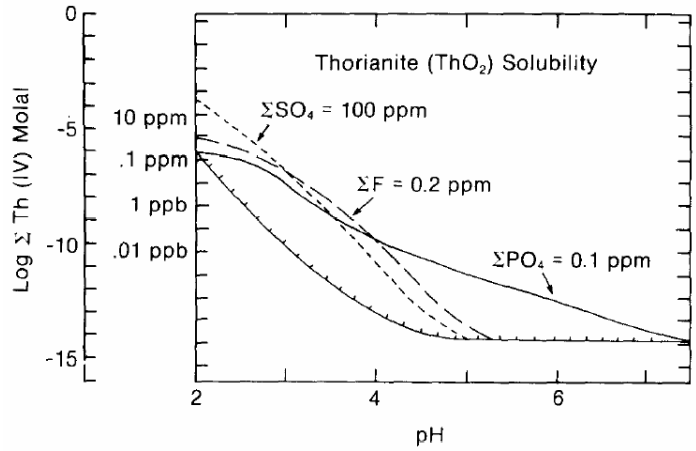

Figure 2: Solubility of thorianite, ThO_2, as a function of pH at 25^{O}C in pure water (lower curve) and in the presence of sulfate, fluoride and phosphate. From Langmuir and Herman (1980)

The solubility of uranium (U) minerals such as uraninite and schoepite also greatly increases under acid conditions. As with thorium, this is driven by the formation of complexes, particularly with fluoride and to a lesser extent, sulfate. Uranium solubility increases by five orders of magnitude at pH of 2 and with dissolved fluoride levels at 2 mg/L (Langmuir, 1978). Under acid conditions, uranium adsorption notably onto iron oxyhydroxides is also inhibited (Hsi and Langmuir, 1985). This increased mobility of uranium under acid conditions forms the basis of the in situ leach (ISL) method of uranium mining where sulfuric acid is used.

This means that the acid sulfate soil environment has many of the preconditions for the dissolution and mobilisation of thorium and uranium from the soil profile. Groundwaters in these areas are characterised by high acidity (pH < 3) with high levels of acid products such as sulfate. The organic rich nature of these swampy landscapes would infer relative enrichment of organic complexes such as oxalates and citrates. Flushing of thorium from the soil profile would occur by the same processes controlling the export of similar acid products (such as sulphate, aluminium and iron). Soil hydraulic conductivity can increase significantly due to the soil ripening process associated with the development of actual acid sulfate soils. In one study, slug test measurements of shallow piezometers measured hydraulic conductivities in the upper oxidised zone that were 2-3 orders of magnitude higher than the deeper unoxidised potential ASS horizon (Brodie et al, 2005). This enhanced permeability can allow an effective transport mechanism within the soil profile to drains, when the shallow watertable is higher than the drain level (Johnston et al, 2003). In areas with low-permeability soils, shallow groundwater and evaporation can lead to accumulation of acid salts on the land surface. In this situation, export of acid products is dominated by surface water processes as these salts can be readily remobilised during rainfall events and discharged into the drainage network by surface run-off (Johnston et al, 2003). With these mechanisms of thorium dissolution and mobility, shallow (<45cm) long-term actual acid sulfate soils should be represented by very low levels of thorium and uranium concentrations in the radiometric imagery.

One complicating factor is the effect of soil moisture which is also known to reduce gamma-ray counts (Saksena et al, 1974; Carroll, 1981). This is likely to be important, in relation to potential ASS mapping with gamma-ray data, since these soils are commonly associated with swamps. Soil moisture increases soil density causing attenuation of the gamma signal but also

adds a physical component that lacks gamma emission. Experimental data has shown that introducing 45% moisture by weight would reduce gamma counts by about one third compared to a dry soil (Carroll, 1981). Grasty (1997) found that, in a clay soil, an increase in soil moisture saturation from 20% to 100% (approx 30% moisture by weight) decreased thorium counts by about 15%. This effect should be considered when interpreting existing gamma radiometrics data and in the planning of new surveys.

3. Tuckean Swamp Case Study

3.1 Catchment Setting

The Tuckean Swamp is a large coastal wetland complex in the Richmond catchment on the north coast of New South Wales, near Ballina and about 700km north of Sydney (Figure 1; Figure 3a). It is a concave swampy depression of about 5,000 hectares in area and mostly at or near 1m AHD in elevation (Morand, 1994). Isolated bedrock hills such as Cedar Island and Paffs Hills rise above the flat landscape. Tuckean Island is a central low sandy rise, surrounded by the back swamp depressions. The swamp is bounded to the north by the elevated basalt flows of the Alstonville Plateau, and to the east by the Blackwall Range.

Geologically, the Tuckean Swamp is a large back barrier lagoon infilled with Quaternary coastal sediments (Drury, 1982). This includes a relatively thick sequence of Pleistocene marine sands and estuarine clays at depth, overlain by a veneer of Holocene estuarine clays and alluvial silts and clays. The nature and distribution of the Holocene estuarine clays is particularly critical as they are pyritic and have the potential to develop into acid sulfate soils. The soils in the swamp have been described as poorly drained humic gleys, gleyed podsolic soils and dense clays (Morand, 1994).

The hydrology of the swamp is highly modified due to construction of drains and a tidal barrage. These works were undertaken to manage frequent flooding of the swamp, either due to local runoff from the upland plateau, or from mainstream flooding from the Richmond River. Drainage commenced in the 1880's with the realignment, straightening and deepening of the natural watercourses. In 1971, the Bagotville Barrage was installed to control the ingress of tidal saline water from the Tuckean Broadwater. With the barrage limiting estuarine influences, the swamp is dominantly a freshwater wetland regime. These works have reduced the period of inundation but it has been estimated that the shallow watertable has declined on average by 0.6m (Christiansen, 1988). The area is considered a major exporter of acid into the Richmond River estuary, via the Tuckean Broadwater (Tulau, 1999a).

3.2 Analysis of Radiometric Data

The airborne thorium data could be compared against the acid sulfate soil risk mapping that is available for NSW coastal regions (Naylor *et al*, 1998). Soil sampling has confirmed significant areas of acid sulfate soils in the Tuckean Swamp as outlined in the risk mapping (Figure 3b), particularly in the lower backswamps and estuarine landscapes (Naylor 1997; Smith *et al*, 1995). The risk mapping presents the probability of the occurrence of acid sulfate soils at various depths in the soil profile. In Figure 3(b) there are areas identified in the swamp with high probability of acid sulfate soils at the surface (red), within 1-metre of the surface (dark purple) and below 1-metre of the surface (light purple).

The gamma-radiometrics imagery for the Tuckean Swamp is shown in Figure 3(c) to (e), with blue representing high concentrations and red representing low, to accentuate low-value anomalies. Figure 3(f) is an ASTER satellite image that shows the land surface reflectance in the visible and near infrared (VNIR). The most important component of the gamma-ray data for understanding soil acidity is the thorium concentration image (Figure 3d) and this is discussed further below.

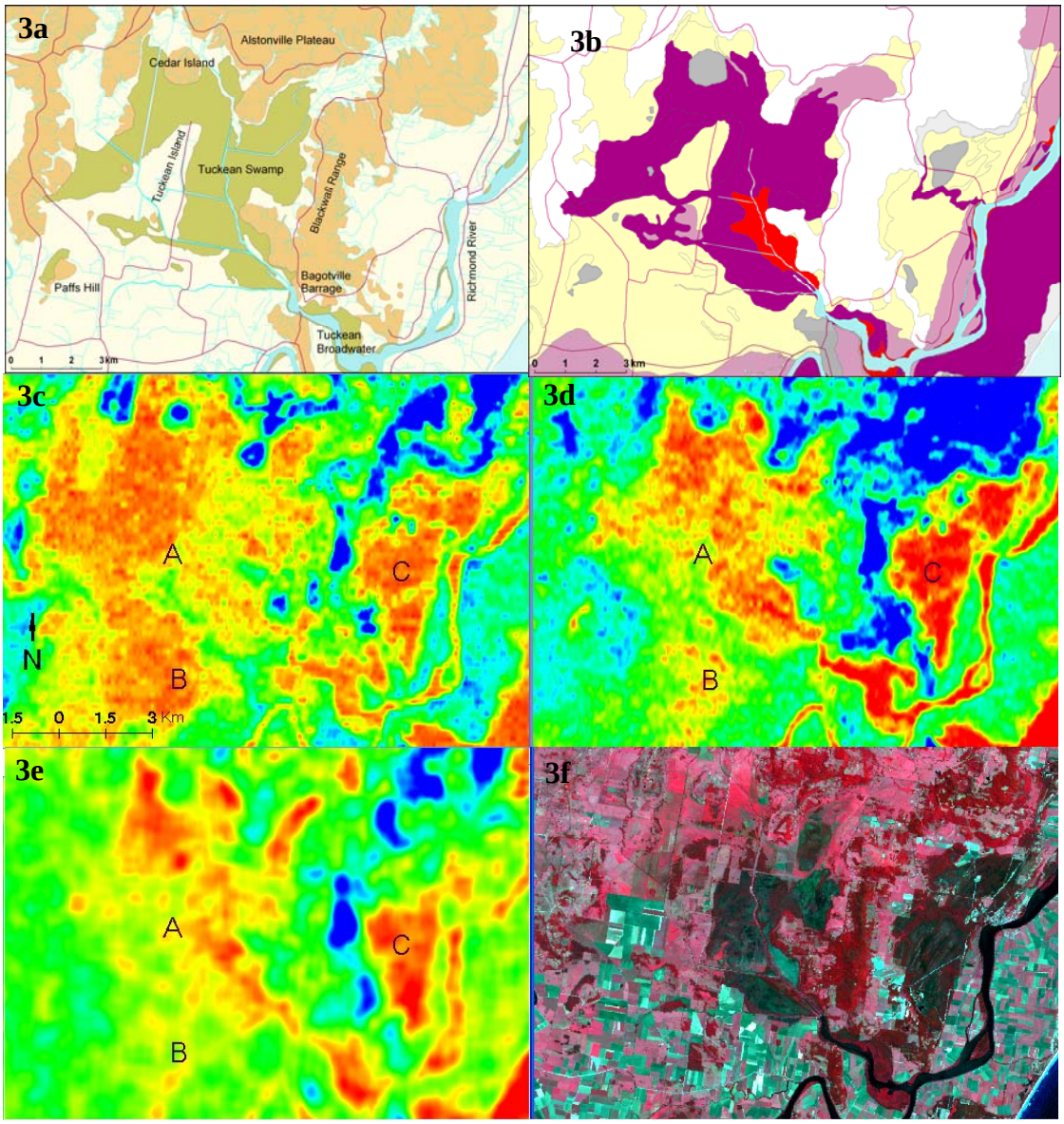

Figure 3. Tuckean Swamp case study area **(a)** Location map showing swamp area (green) and post-Quaternary geology (orange) **(b)** Simplified acid sulfate soil risk map (after Naylor, 1997) with high probability of ASS at or near the surface (red), within 1 metre of the surface (dark purple) and below 1 metre of the surface (light purple). Also low probability areas (yellow) and areas not assessed such as no known occurrence or disturbed terrain (grey). Airborne gamma-ray (radiometrics) image data displayed with a rainbow colour scale (blue is high and red is low) for **(c)** potassium with range cut-offs of 0 – 0.75% **(d)** thorium with range of 0.5 – 6.5 ppm and **(e)** smoothed uranium with range of 0.1 – 1.8 ppm **(f)** ASTER satellite VNIR data with bands 3, 2 and 1 displayed as RGB – red indicates high near infrared reflectance of healthy vegetation

Overall, the swamp has relatively low concentrations of potassium (Figure 3c). However, there is limited consistency with the risk mapping, as the lowest values (red) occur in both high risk backswamps, as well as more elevated areas designated low risk due to the presence of sand cover, such as in the Tuckean Island (A in Figure 3) and Green Forest (B in Figure 3) areas. The high potassium (green and blue) zone bordering the Richmond River is interpreted to be modern alluvial floodplain deposits. These deposits are inferred to be thin (<1-3m) as these areas are also designated as high risk in the acid sulfate soil mapping. Part of this thin alluvial cover appears to extend up into the Tuckean Swamp, towards Tuckean Island.

The thorium imagery (Figure 3d) shows a striking correlation with the risk mapping, with very low thorium values (red) matching high risk areas (highlighted as red and dark purple in Figure 3b). Thorium depletion to levels less than about 3-4 ppm in these areas is consistent with thorium being mobilised in an acidic, sulfate- and organic-rich environment. In this context, the lower values (red in Figure 3d) within the swamp are interpreted to be areas of long-term shallow actual acid sulfate soils. Scattered anomalies with similar thorium levels are evident in the Green Forest area (B) and warrant further investigation. The thorium lows coinciding with the Richmond River and Tuckean Broadwater are due to blocking of the gamma-ray signal by these water bodies. The consistent thorium low evident in the coastal floodplain east of the Blackwall Range (C) is associated with marine sand deposits interpreted to have no heavy mineral assemblages. These anomalies highlight the fact that gamma-ray signatures often overlap for different materials and that the thorium imagery should be carefully interpreted with local knowledge of water cover and regional geology.

The uranium imagery (Figure 3e) for the swamp has been smoothed using an average filter (7 x 7 kernel) to remove spatial noise due to the typical low uranium counts. This results in the uranium image showing considerably less detail. However, similar to thorium, the uranium lows (red) in the swamp correspond with the areas mapped as high probability of acid sulfate soils within 1-metre of the land surface (red and dark purple in Figure 3b). This also suggests that these are areas of dissolution associated with long-term acid conditions. Also, like the thorium signal, low uranium values can also be associated with water bodies and marine sands. Uranium appears to have potential for mapping soil acidification, but using ground-based gamma survey methods that record better resolution signals rather than from airborne methods.

3.3 Field Measurements

On-ground measurements were taken in the Tuckean Swamp using a portable spectrometer to confirm the relationship between the low thorium signal and acidification. Measurement sites corresponded with the locations of piezometers or monitoring bores to allow simultaneous measurement of the acidity of the shallow groundwater. A few of the measurements were taken in November, 2004 following rainfall and were in the vicinity of inundated areas (2-5cm water depth). However, no ground measurement sites actually had water cover. Follow up measurements in March, 2005 were during dry conditions when no standing water was present in the vicinity of these sites and the soils were not fully saturated in the near-surface.

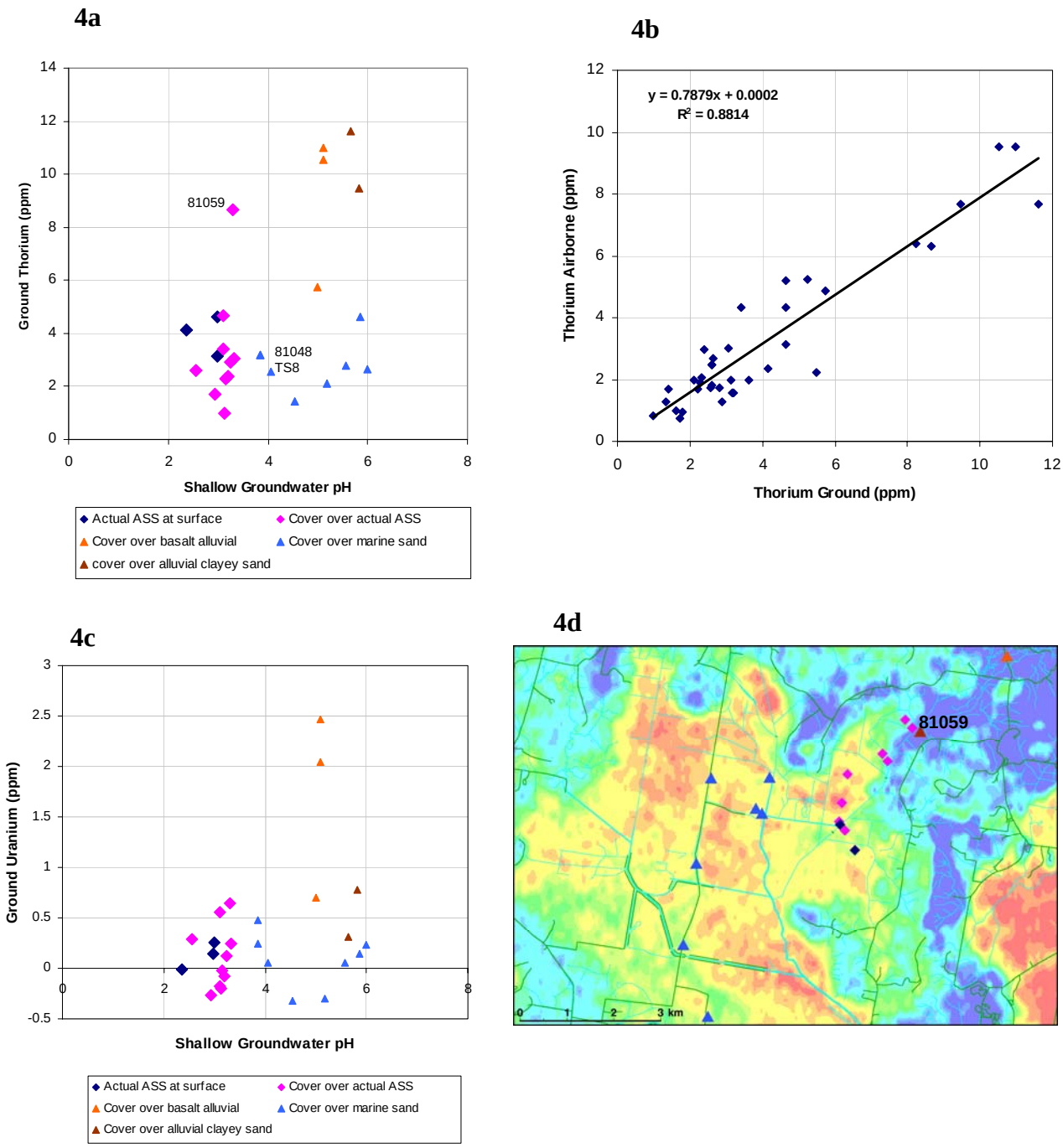

Figure 4. Field measurements of thorium and uranium in the soil profile and pH in shallow groundwater in the Tuckean Swamp **(a)** Correlation between ground-based ppm thorium and shallow groundwater pH **(b)** Correlation between ground-based and airborne measurements of thorium **(c)** Correlation between ground-based ppm uranium and shallow groundwater pH and **(d)** location of field measurement sites relative to airborne thorium image (red = low)

Recognising the stratigraphic differences across the swamp, these sites were categorised based on the available lithological logs into having either:

(i) Actual acid sulfate soil exposed at the surface;
(ii) Actual acid sulfate soil at depth with variable cover (0.2-0.8m) of typically black, peaty clay floodplain soil;
(iii) Basalt derived alluvial or colluvial material with cover (0.4-0.5m) of floodplain clay soil. No acid sulfate soil evident in the shallow profile;
(iv) Quartzose marine sand with variable cover (0-1.5m) of floodplain clay soil;
(v) (Meta)sediment derived(?) alluvial clayey sand material with cover of floodplain soil.

The relationship between the ground-based thorium measurements and shallow groundwater acidity is presented in Figure 4(a). The sites with actual acid sulfate soils within the soil profile and acid shallow groundwater generally had low on-ground thorium measurements. The lack of standing water and significant near-surface soil moisture at the time of field measurement suggests that attenuation of the gamma-ray signal by water cover is not the principal cause for the low-thorium response in the airborne survey over the Tuckean Swamp. Rather, the association with shallow groundwater acidity suggests that dissolution and mobilisation of thorium has occurred at these sites. The mechanism for thorium removal from the soil profile would be that it is removed with the flushing of acid water that is known to occur in acid sulfate soils.

The acid sites have variable cover of floodplain material overlying the actual acid sulfate soil horizon. The acid site with the anomalously high thorium levels in Figure 4a (Site 81059) had a relatively thin actual acid sulfate soil layer (0.2m) and had the thickest cover of floodplain material (0.8m), or about double the soil thickness considered to be the gamma-ray source. This site is also located marginal to a zone interpreted to have metasediment derived alluvial cover with higher thorium activity, highlighted as blue in Figure 4d. It is likely that some of this material is also within the surface cover at site 81059, and the main source of the relatively elevated thorium signal.

The remainder of these acid sites had cover varying between 0-0.6m, which was typically black, peaty clay soil. The low-thorium signal is not impeded by this floodplain cover, which can exceed the accepted depth of penetration associated with gamma-ray spectrometry (0.3-0.5m). It is inferred that at these sites the shallow and fluctuating watertable has allowed acid groundwater to migrate up into this floodplain cover and remove the thorium from this material.

Figure 4(a) also highlights the issue of using the thorium signal to differentiate actual acid sulfate soils from other landscape units. In particular, sites dominated by marine sands in the soil profile also have low thorium concentrations but are more moderate in terms of acidity, with pH values typically between 4 and 6. The more acid of these sites (81048 and TS8) are located close to the main drain and have relatively high groundwater salinities suggesting tidal ingress of brackish acid drain water. The general low-thorium response for the marine sands highlights the need for identifying and masking out this geological unit as part of the mapping process. This is possible using other datasets including existing geological mapping as demonstrated in the method presented in the chapter following. The sites in the upper reaches of the swamp dominated by basalt- or metasediment-derived material and with no indications of acid sulfate soils tend to have higher thorium values.

As expected, Figure 4(b) shows the strong linear relationship between the airborne and on-ground thorium measurements. This is not a 1:1 relationship mainly because of the contrast in the domain being sampled, as the airborne survey has a footprint of about 100m diameter, whilst the ground measurements have a footprint of about 5m diameter. This means that the

airborne survey aggregates the signal for a much larger area. Also the absolute values from the two different instruments are likely to be different due to errors in sensitivity calibration in either or both of the sensors used.

Although constrained by the limited number of site measurements, information from these two figures can be combined to estimate thresholds for mapping purposes. From Figure 4a, the sites with near-surface actual acid sulfate soils had groundwater pH < 3.4 and on-ground thorium concentrations < 4.7ppm. This thorium value corresponds to an airborne survey value of 3.7 ppm (Figure 4b). This suggests that a threshold of about 3-4ppm could be used as one of the criteria for processing the airborne data to highlight intense soil acidification.

The relationship between the on-ground uranium measurements and shallow groundwater (Figure 4c) is similar to that for thorium. The negative values for the ground uranium data indicate a calibration problem with the field spectrometer. Despite this, all of the actual acid sulfate soil sites had relatively low levels of uranium, supporting dissolution and mobilisation in these conditions. However, other landscape units not associated with extreme acid conditions, such as marine sands also had similar uranium values. In particular, there is less differentiation between the acid sulfate soils and the alluvial clayey sands in the uranium measurements, compared with the thorium measurements. This, combined with the generally noisy airborne uranium imagery, makes thorium a better candidate for mapping acid sulfate soils.

4. Remote Sensing and GIS Modelling of Surface Soil Acidity

As shown in the previous chapter, the thorium concentration imagery provides an indicator for surface acidity in the Tuckean swamp area, albeit not a complete and independent one. Given that the airborne gamma-ray survey covers a significant section of the northern NSW coast, it is possible to attempt rapid remote mapping of shallow actual acid sulfate soils at a regional level.

The thorium concentration image for the whole survey is presented in Figure 5, compared with the ASTER VNIR data. Like the thorium imagery for the Tuckean Swamp (Figure 3d) red represents low values and blue represents high, to highlight the low-thorium anomalies. Extrapolating the simple relationship described for the Tuckean Swamp to the regional scale is problematic due to the presence of the other sources of very low thorium. In the Clarence and Richmond catchments, these are mainly water bodies and areas of quartz sand cover (commonly beach ridge deposits) along the coast as recognisable in Figure 5a. There are other smaller low thorium sources in bedrock areas such as basalt and sandstone outcrops. The focus for a GIS-based approach for mapping soil acidification is to develop a methodology to separate out these areas. A number of datasets, independent of the thorium concentration data, can be used to help identify and mask these non-acid low-thorium anomalies. These datasets and their application in the model are described below.

4.1 Digital Elevation Model (DEM)

The DEM was acquired simultaneously with the airborne geophysics by laser altimetry (Mitchell & Minty, 1998). Bedrock sources of very low thorium, although minor in extent, were excluded by applying a mask for elevations above 15m AHD. Although acid-sulfate soils in Holocene estuarine sediments are unlikely to occur at elevations above 10m AHD, the higher value was used because it was evident that the altimetry data could be measuring tree-tops rather than the land surface. Although slightly arbitrary, the threshold appeared to be effective in delineating the alluvial and estuarine landscapes from the bedrock upland areas.

4.2 Satellite ASTER Data

Solar reflective and thermal satellite data was acquired from the Advanced Spaceborne Thermal Emission and Reflection radiometer (ASTER). Data from this platform has the advantage of being available in the public domain at very low cost. Included are 3 bands in the visible and near-infrared (VNIR), 6 bands in the short-wave infrared (SWIR) and 5 bands in the thermal infrared (TIR) at spatial resolutions of 15m, 30m and 90m respectively, refer Table 1. ASTER operates in two distinct spectral regions: the solar reflective (VNIR and SWIR bands) where the measured radiance is reflected solar radiation, and the TIR where radiance is due to thermal emission.

In a potential model, the SWIR data can be used to identify water bodies since even shallow water efficiently absorbs radiation in this part of the spectrum. This means that a threshold value can be applied that effectively masks water bodies from the thorium data. One potential problem is the difference in spatial resolution between the two datasets – ASTER SWIR is 30m whereas the thorium data have 50m pixels although the non-directional “footprint” is more like 100m. The effects of this resolution difference are discussed later.

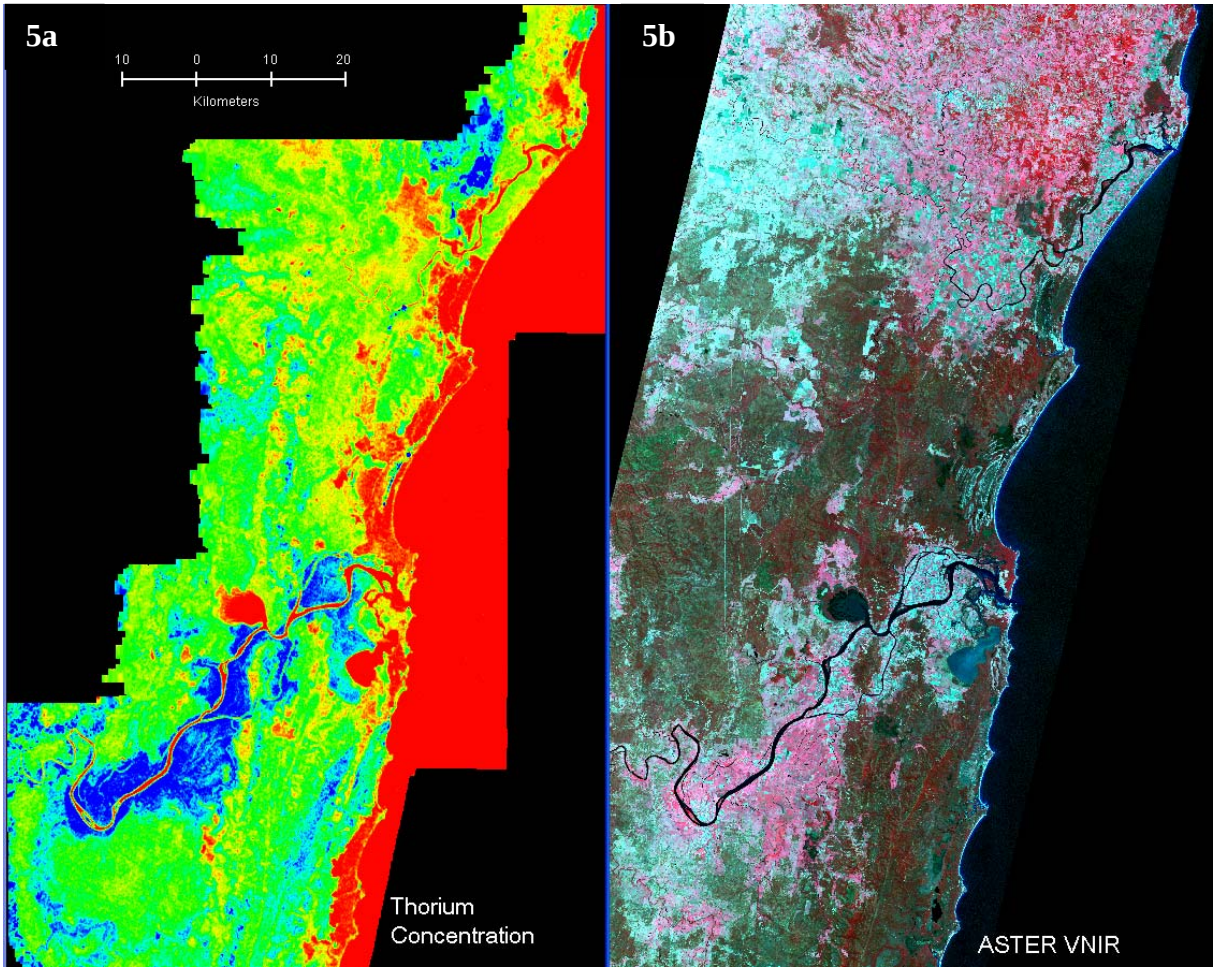

Figure 5. NSW north coast geophysical survey area **(a)** Thorium concentration with "rainbow colour table applied" to the data range of 1 ppm (red) to 10 ppm (blue) **(b)** ASTER bands 3, 2 and 1 shown as red, green and blue respectively. Red colours indicate high near infrared reflectance associated with healthy vegetation

Table 1: ASTER wavebands

Spectral Range	Band	Wavelength (micrometres)
VNIR	1	0.52 – 0.60
	2	0.62 – 0.69
	3	0.76 – 0.86
SWIR	4	1.60 – 1.70
	5	2.145 – 2.185
	6	2.185 – 2.225
	7	2.235 – 2.285
	8	2.295 – 2.365
	9	2.360 – 2.430
TIR	10	8.125 – 8.475
	11	8.475 – 8.825
	12	8.925 – 9.275
	13	10.25 – 10.95
	14	10.95 – 11.65

The TIR data can provide information about the location of quartz sands since quartz has characteristic emissivity features in the spectral range of the ASTER TIR bands. The approach that can be used is the "decorrelation stretch" (Gillespie, 1992) using bands 10, 12 and 13 (see Table 1) where the emissivity properties are effectively enhanced and the obscuring, band-correlating effects of temperature are removed. Due to the relative lows in quartz emissivity in bands 10 and 12, a threshold applied to the decorrelated band 13 provides an index of the quartz content. However, this will only be successful in areas that are largely unvegetated since vegetation emission will mask the quartz signature. This is likely to be a factor in the Clarence-Richmond area so that additional means of locating and masking the low-thorium quartz sand units are needed.

Three adjacent ASTER scenes (each 60 x 60 km) on the same path and dated 11 November, 2003 were acquired. No ASTER imagery is available for the time of the geophysical survey as the satellite was only launched in December, 1999.

4.3 Geological Mapping

Recently completed Quaternary geological mapping sourced from the NSW Geological Survey (Troedson and Hashimoto, 2005) provided a solution to the identification of low thorium due to quartz sand cover and hence non-acid soils. Extensive marine sand areas near the coast have been accurately mapped as a coastal barrier system and the geological units making up this landscape provide an effective mask for the acid model. Table 2 shows the geological units dominated by quartzose marine sands that were identified as suitable for the masking procedure.

In many coastal regions, such comprehensive Quaternary geology mapping may not be available and alternative methods would be required to identify quartz sand deposits. To overcome this problem, the ASTER VNIR data could be used as a base to visually interpret the boundaries of the beach ridge deposits. This is feasible due to the often identifiable linear and curved structure of the beach ridges although some areas of sand deposits (such as dunes or barrier flats) may not be distinguishable. As discussed above, decorrelation stretch of thermal infrared ASTER data can also be used to assist in identifying quartz rich areas.

4.4 The Stepwise Classification Model

To generate a GIS-based map of surface soil acidity based on the thorium imagery, data sets described above were input to a simple stepwise classification scheme:

If **ASTER SWIR Band 4** < DN 33 then **CLASS 6**
Else If **DEM** > 15 then **CLASS 5**
Else If **GEOLOGY** = Coastal Barrier Sand units (see Table 2) then **CLASS 4**

After identification and masking of areas that cannot be acid-sulfate, the thorium image was then split into three classes:

Else If **THORIUM** > 3.5 ppm then **CLASS 3**
Else if **THORIUM** > 2 ppm then **CLASS 2**
Else if **THORIUM** <= 2 ppm then **CLASS 1**

Table 2: Quaternary marine sand geological units used in GIS analysis (from Troedson and Hashimoto, 2005)

Depositional System	Geological Symbol	Age	Geological Unit	Lithologies
Coastal Barrier	Qhbb	Holocene	sandy beach	marine sand, shell, gravel
	Qhbbg	Holocene	gravel beach	gravel, shell, marine sand
	Qhbd	Holocene	dune	marine sand
	Qhbdm	Holocene	mobile dune	marine sand
	Qhbdr	Holocene	bedrock-mantling dune	marine sand
	Qhbf	Holocene	back barrier flat	marine sand, silt, clay, gravel, shell
	Qhbr	Holocene	beach ridge and associated strandplain	marine sand, shell, gravel
	Qhbw	Holocene	beach ridge swale and dune deflation hollow	marine sand, organic mud, peat
	Qhs/Qpbw	Holocene	freshwater swamp in beach ridge swale and dune-deflation hollow	marine sand, indurated sand, organic mud, peat
	Qpb	Pleistocene	undifferentiated coastal barrier	marine sand, indurated sand
	Qpbd	Pleistocene	dune	marine sand, indurated sand
	Qpbdr	Pleistocene	bedrock-mantling dune	marine sand, indurated sand
	Qpbf	Pleistocene	back barrier flat	marine sand, indurated sand, silt, clay, gravel, organic mud, peat
	Qpbr	Pleistocene	beach ridges and associated sand plain	marine sand, indurated sand, gravel
	Qpbr1	Pleistocene	beach ridges and associated sand plain (set 1)	marine sand, indurated sand, gravel
	Qpbr2	Pleistocene	beach ridges and associated sand plain (set 2)	marine sand, indurated sand, gravel
	Qpbw	Pleistocene	beach ridge swale and dune-deflation hollow	marine sand, indurated sand, organic mud, peat
Estuarine Plain	Qpef	Pleistocene	tidal-delta flat	marine sand, silt, minor clay, indurated sand, shell

4.5 Model Results

The results of this classification for the entire survey area are shown in Figure 6a. The model has identified many of the known acid hotspots as identified by the acid risk mapping (Figure 6b), as well as providing important new information. Figure 5 also highlights a fundamental difference in the two mapping approaches. The risk mapping indicates the probability of the existence of acid sulfate material at various depths within the soil profile, encompassing both actual and potential acid sulfate soils. This has a broader scope than the thorium-derived model which only maps long-term and shallow (<0.45m) actual soil acidification. Class 1 (red) and 2 (orange) of the thorium model (Figure 6a) should only correlate with actual acidification within the near-surface high risk category (red, Figure 6b) and a shallow part of the high risk category within 1 metre of the surface (dark purple, Figure 6b). The model does not identify potential acid sulfate soils that have not been disturbed or actual acid sulfate soils with thick non-acid cover. The model would also not detect recently activated shallow acid sulfate soils where thorium depletion has not yet occurred.

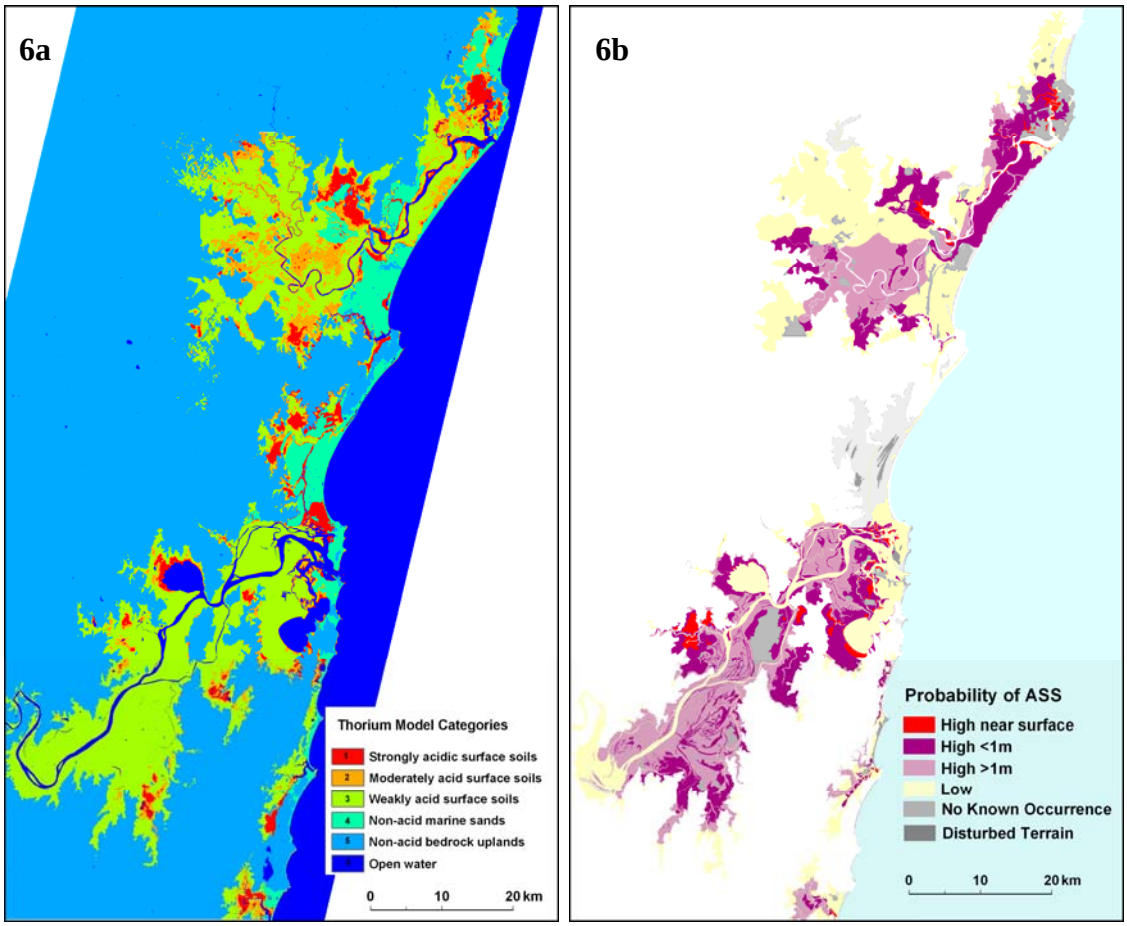

Figure 6. Comparison of thorium model and existing acid risk mapping
(a) Results of stepwise classification of gamma-ray thorium, DEM, geology, and ASTER data. The classes represented are described as follows:

(1) strongly acidic surface soils, minor false inclusion errors of sandy soils
(2) medium acidic surface soils
(3) low acid surface soils
(4) sandy soils from existing geology mapping
(5) Areas higher than 15m elevation
(6) Open water

(b) Simplified DIPNR acid sulfate soil risk mapping (Naylor *et al*, 1998) with high probability of ASS at or near the surface (red), within 1 metre of the surface (dark purple) and below 1 metre of the surface (light purple). Also low probability areas (yellow) and areas not assessed such as no known occurrence or disturbed terrain (grey)

The model output and the risk mapping were compared more closely for specific parts of the survey area. Revisiting the Tuckean Swamp shows a good correlation between the thorium model and the risk mapping (Figure 7). The risk mapping indicates a high probability of acid sulfate material at or near the surface (red), within 1 metre of the surface (dark purple) and below 1 metre of the surface (light purple) while the thorium model identifies large areas of shallow acid soils to a depth of 30-45 cm. Therefore it is inferred that most of the "high risk < 1 m" zone for the Tuckean Swamp is associated with actual acid sulfate soils within the top 30-45 cm.

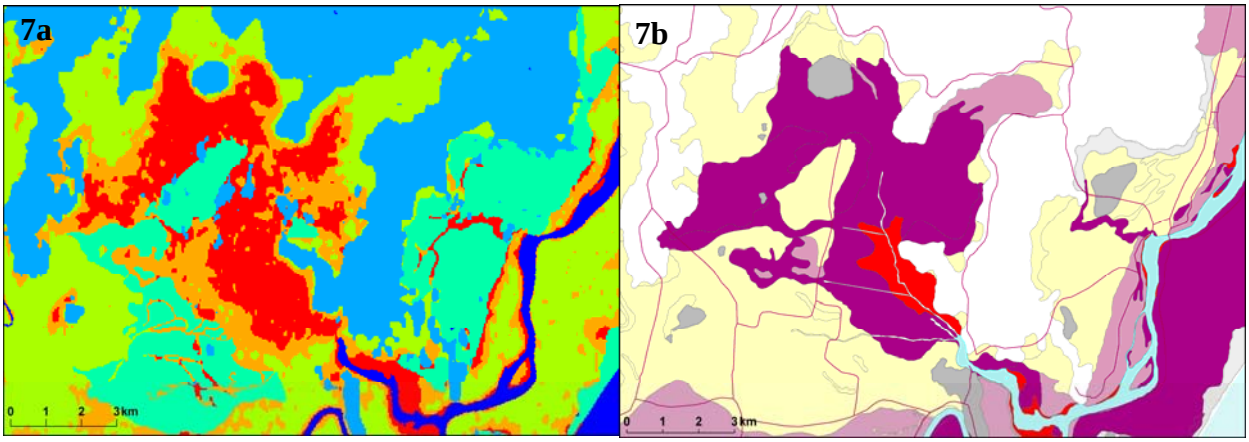

Figure 7. Comparison of **(a)** thorium model output (see Figure 5 for description of categories) with **(b)** DIPNR acid risk mapping at the Tuckean Swamp "hotspot"

Near the outlet of the Richmond River, the soil acidification defined by categories 1 (red) and 2 (orange) of the thorium model (Figure 8a) encompasses all of the "high probability near surface" (red) category and part of the "high probability <1m" (dark purple) risk category (Figure 8b). In this way, the thorium data can differentiate the latter risk category into two separate zones relating to (1) shallow actual acidity and (2) the presence of potential acid sulfate soils or shallow cover above actual acid sulfate soils. This is confirmed by the potassium imagery (Figure 8c) where high potassium levels (green-yellow-red) bordering the Richmond River (e.g. area B) correspond to floodplain alluvial, while such cover appears to be non-existent for the area interpreted to be acidified to the north (area A), which has low potassium levels (blue), although this could partly be due to increased water saturation.

The thorium model identified a number of acid anomalies in the mid-coastal section of the survey area (Figure 9). One of these is a known hotspot (area A in Figure 9a) while others, for example the areas near sites B and C, are unlikely to be acid sulfate zones, being mapped as freshwater swamps containing organic mud, peat clay silt and marine sand underlain by undifferentiated Pleistocene sediments (Troedson & Hashimoto, 2005). This geomorphology is also indicated by the ASTER VNIR data (Figure 9d) which shows that areas B and C are dark toned, lacking in vegetation and different to the adjacent quartz sand beach ridges to the east. These areas are also not indicated as quartz rich areas in Figure 9c, an image derived from decorellation stretching of the ASTER TIR data. The most likely explanation for the low thorium in these areas is that the lakes had water cover at the time of the airborne gamma survey, although it is not possible to confirm this with the acquired data sets. Rainfall records show that there had been more rain prior to the gamma survey than prior to the ASTER scene. However, imagery identification of the presence of water at the time of the gamma survey is complicated by the fact that this survey was conducted intermittently over several months. The interpretation of water rather that acidity is also supported by the lack of iron-oxide products at the surface, as indicated by unmixing of Landsat TM (Bierwirth & Graham, 1998).

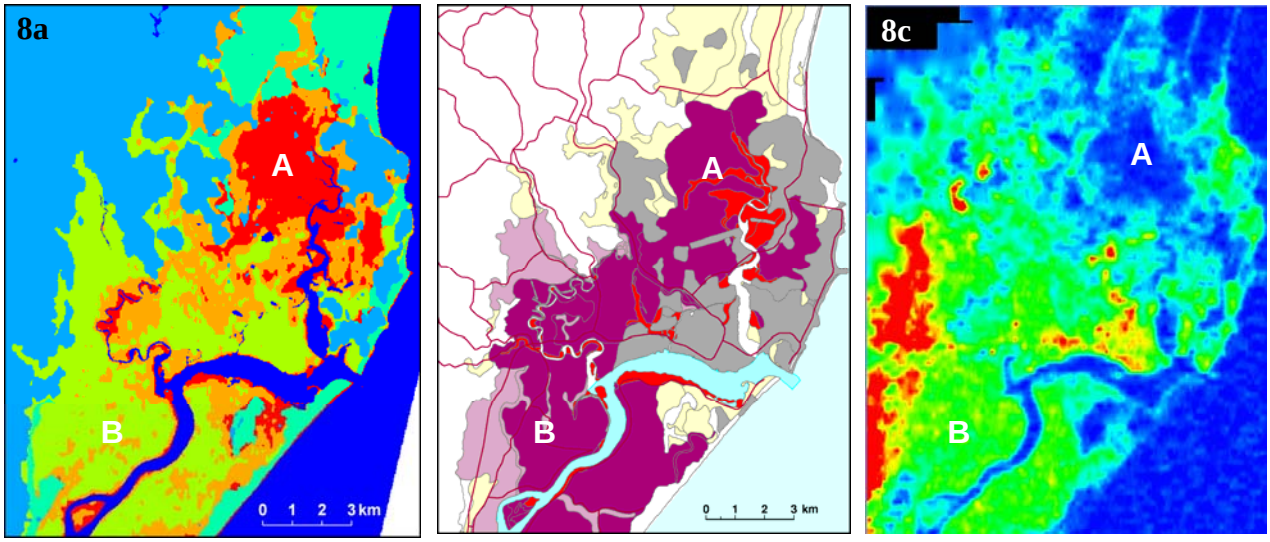

Figure 8. Comparison of **(a)** thorium model output with **(b)** DIPNR acid risk mapping and **(c)** potassium concentration (red = high) at the "hotspot" near the Richmond River outlet

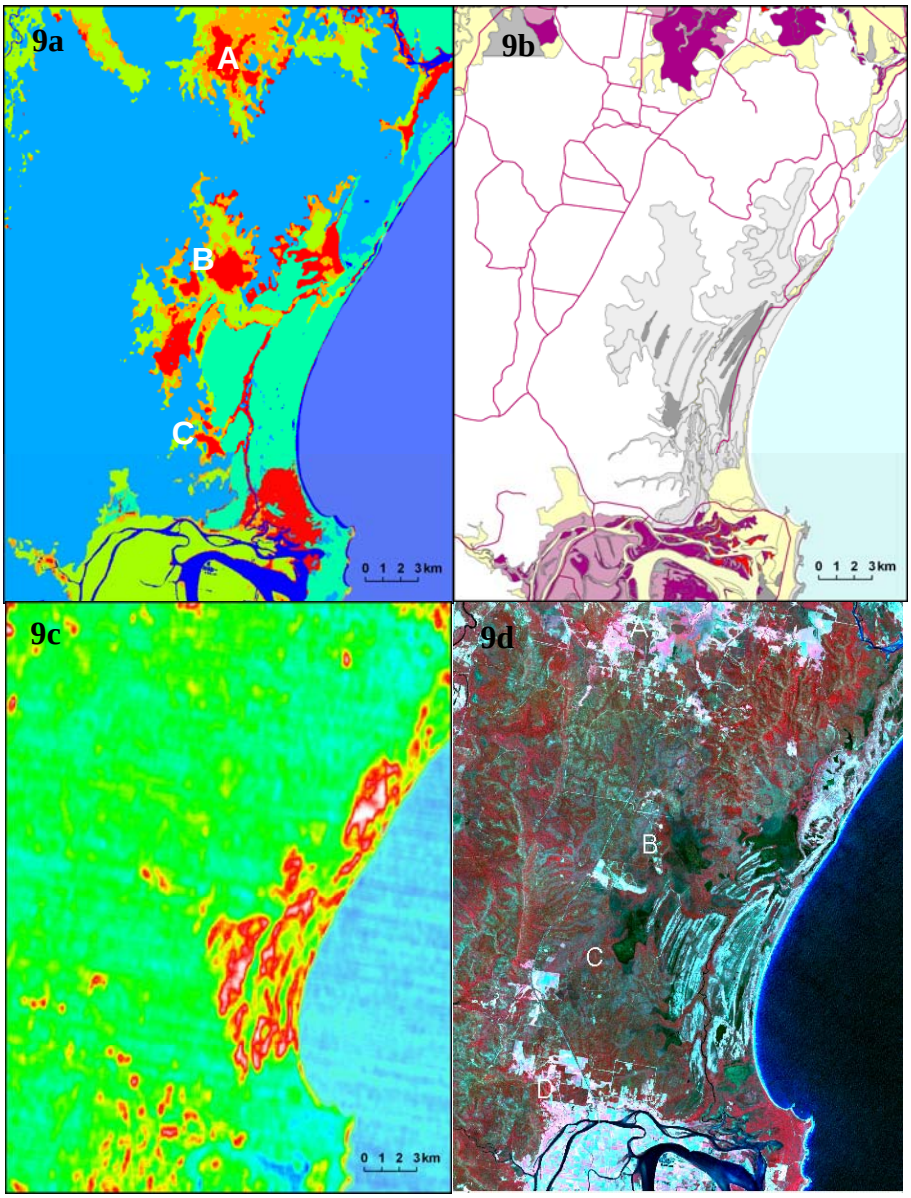

Figure 9 Comparison of **(a)** thorium model output with **(b)** DIPNR acid risk mapping **(c)** quartz unmixing from ASTER TIR band (red = high quartz) and **(d)** ASTER VNIR bands 3, 2 and 1 shown as RGB respectively, for area north of the Clarence River outlet

Along the Clarence River, the thorium model (Figure 10a) delineated the areas within the high acid risk classes (Figure 10b) that are likely to have the strongest acidity at the surface. In the floodplain, the potassium imagery (Figure 10c) indicates recent deposition of silts, verified in the field to correlate with the depth of alluvial cover overlying potential acid sulfate soils (Bierwirth and Graham, 1998). In red areas on the potassium image, alluvial cover can be greater than 2m. The potassium image shows that area A is likely to have alluvial cover at the surface, even though the acid risk mapping shows high acid risk at the surface (Figure 10b). This alluvial cover would explain why this area is not delineated as having strong surface acidification by the thorium model (Figure 10a). In contrast, the low potassium signal for the area at B suggests minimal alluvial cover and the thorium model shows strong acidity at the surface. This relationship also holds for the Shark Creek hotspot, where the northern half (area C) appears to have alluvial cover that is absent in the southern half (area D) which is strongly acidified at the surface. At least part of the low thorium response at areas B and D could be due to the presence of moisture as indicated by the low response of the ASTER SWIR data although the extent of this influence is unclear. In general, this information is valuable for land management in this area.

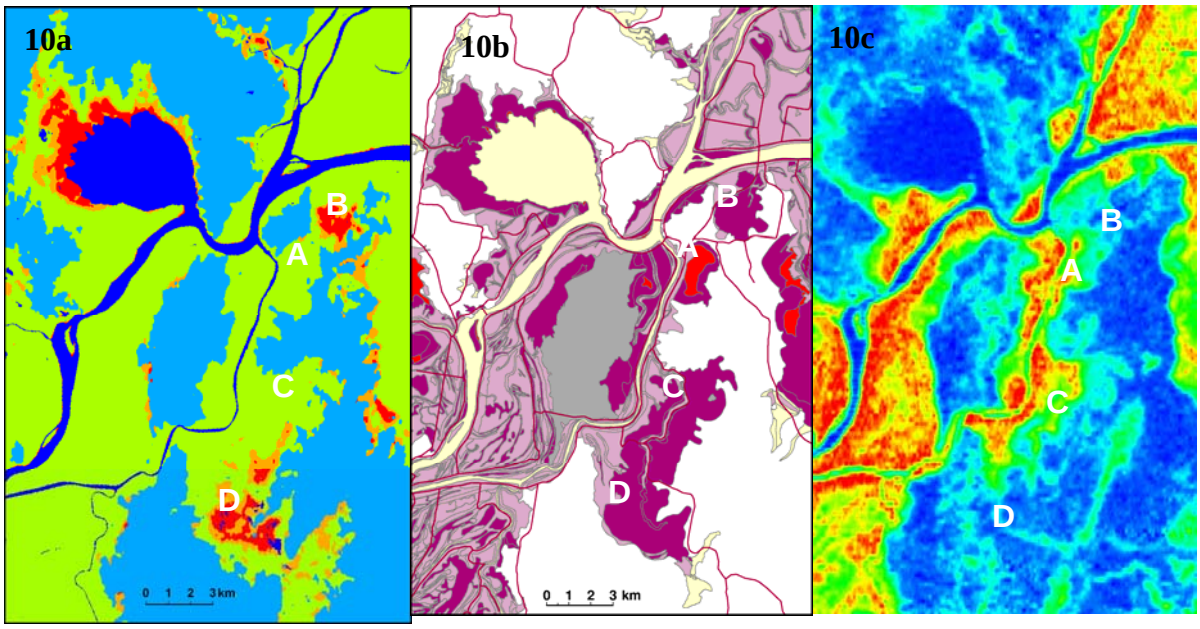

Figure 10. Comparison of (a) thorium model output with (b) DIPNR acid risk mapping at (c) potassium concentration (red = high) for the Clarence River area

5. Discussion and Conclusions

Analysis of field gamma spectrometer data, existing mapping and satellite image data indicates the usefulness of thorium image concentration data to target areas of long-term intense acidification in the top 30-45 cm of the soil profile. Low concentrations of thorium in acid areas are due to the mobilisation of the element by acidic groundwater promoting complexing with sulfate, fluoride and organic ligands. Although the gamma-ray signature is not unique, it is demonstrated here that other remote sensing and map layers can be used in a GIS-based model to exclude non-acid low-thorium anomalies.

The method used is a simple but appropriate use of thresholds on data layers to mask areas that are non-acid sources of low thorium concentration. The model is not perfect however due to various effects. Inaccuracies are present in the DEM sourced from the geophysical survey due to the radar altimeter taking readings from the tops of trees, rather than the land surface. This will affect the accuracy of the DEM derived boundary for potential acid sulfate soils. Residual low-thorium anomalies may also occur at the edge of water bodies due to the use of the ASTER SWIR data to mask water bodies, which has a finer spatial resolution than the airborne radiometrics data. This effect can be seen along the edge of the Richmond River in Figure 8a. As the radiometric data and ASTER data were collected at different time periods there is also the potential mismatch between the distributions of water cover. This has apparently resulted in the modelled identification of acid areas within non-acid freshwater swamps as shown in Figure 9. Another issue is that the radiometric survey was flown over two time intervals within a seven-month period. Ideally, multiple SWIR datasets correlated with the actual time of gamma radiometric surveying are required to characterise water cover. It is recommended that radiometric surveys be flown in the coastal zone during relatively dry periods, and that synchronous remote sensing data be used.

Apart from water cover, soil moisture is a factor that may affect the gamma signal but cannot be readily masked since acid sulfate areas are commonly associated with swamps or high soil moisture. As previously discussed, soil moisture changes from dry to fully saturated could reduce thorium values by about a third. While this means that some thorium value changes in ASS areas will relate to moisture rather than pH variations, it is unlikely that moisture-saturated non-acid soils will be falsely identified. Examples of lower thorium responses in ASS hotspots associated with increased moisture are areas at A in Figure 8 and D in Figure 10. Despite this complication, the method of identifying low-thorium anomalies is still valuable in targeting ASS hotspots and again the acquisition of gamma-ray data during dry periods will reduce this problem.

Another potential problem in the general application of the method is that thorium concentration is identical in many areas for both acid soils and non-acid quartz sands. The current model uses detailed geological mapping to effectively map and mask sandy areas with low acid potential. However in many areas such detailed geological mapping may not be available and existing maps may be prone to subjective and simplified boundaries. A partial solution would be to create masking layers using the ASTER VNIR data (see Figure 9c) and ASTER TIR quartz index (see Figure 9d) although both of these data are limited by thick vegetation cover. A particular complexity is the differentiation of non-acid quartz sands from any sulfidic sands that can potentially generate acid.

The method described here is designed as a simple reconnaissance tool for targeting long-term acid soils in the near surface (<30-45 cm). As such the information is different from and complementary to the existing acid risk mapping (Naylor et al, 1998). The risk mapping identifies the probability of acid sulfate soils (both actual and potential) at various depths (including at the surface and < 1 metre). The thorium model attempts to identify actual acid

soils to a depth of 30-45 cm but not necessarily below this. The thorium data is valuable in that it subdivides the “high risk < 1 m” category into actual versus potential acidity and the presence of alluvial cover.

This work highlights the potential for using airborne radiometric surveys in identifying acid sulfate soil hotspots at a catchment level. This is useful as a targeting tool to highlight the worst areas of intense acidification that require further investigation and to prioritise investment of on-ground works. The methodology is generic as it is based on the mobilisation of thorium in an acid environment, so should be transferable to other coastal catchments. This is significant considering that there is an estimated 13.5 million hectares of acid sulfate soils globally, with 1 million hectares in Australia (White *et al*, 1995). Data from airborne gamma-ray surveys is already available in the public domain for parts of the Australian coastal zone. This is a new application of these surveys and is complementary to the existing methods of mapping acid sulfate soils such as airphoto interpretation and soil sampling. It is cost-effective on a per hectare basis and rapid. It also has the advantages that other geophysical techniques (such as magnetics or electromagnetics) can also be incorporated into any proposed airborne survey and that the radiometrics data can be used for other purposes (such as mapping other soil properties and types).

6. Acknowledgements

This work was initiated as part of the Managing Connected Water Resources Project, focussing on conjunctive water management. The Tuckean Swamp is a trial catchment for the project with work focussing on the acid sulfate soil issue, particularly the interactions between the shallow acid groundwater system and the drain network. The project is collaborative between the Bureau of Rural Sciences, Australian Bureau of Agricultural and Resource Economics, the Australian National University (Centre for Resource and Environmental Studies), NSW Department of Infrastructure Planning and Natural Resources and Queensland Department of Natural Resources and Mines. The Natural Heritage Trust II and the Australian Research Council fund the project. Information about the project is available at http://www.brs.gov.au/connectedwater.

Stephen Hostetler and John Spring (BRS) provided valuable technical assistance in the collection of field radiometric and water chemistry data. The authors also gratefully acknowledge the comments on the original manuscript provided by Professor Ian White (ANU), Dr Peter Slavich (DPI, Wollongbar), Dr Michele Barson (BRS), Richard Green (DIPNR) and Mitch Tulau (DIPNR).

7. References

Aspin SJ and Bierwirth PN. (1997), GIS analysis of the effects of forest biomass on gamma radiometric images. *Proceedings, 3rd National Forum on GIS in the Geosciences.* AGSO Record 1997/36, p77-83. Australian Geological Survey Organisation.

Bierwirth PN. (1997), The use of airborne gamma-emission data for detecting soil properties. *Proceedings of the Third International Airborne Remote Sensing Conference and Exhibition.* Copenhagen, Denmark.

Bierwirth PN and Graham TL. (1998), Remote Sensing of Acid Sulfate Soils using Multispectral and Gamma-ray data. *Proceedings of the 9th Australasian Remote Sensing Conference*.

Brodie RS, Baskaran S and Hostetler S, 2005. Tools for assessing groundwater-surface water interactions: a case study in the Lower Richmond catchment, NSW. Bureau of Rural Sciences, Canberra.

Carroll, T.R., (1981). Airborne soil moisture measurement using natural terrestrial gamma radiation. *Soil Science*, 132(5), pp358-366.

Christiansen K. (1988), A total catchment approach to the management of Tuckean Swamp. *Integrated Project*, University of New England – Northern Rivers.

Drury, L.W. (1982), Hydrogeology and Quaternary stratigraphy of the Richmond River valley. PhD thesis (unpubl.) Dept. Geology, University of New South Wales, 2 vol. 643p.

Gillespie AR. (1992), Enhancement of Multispectral Thermal Infrared Images: Decorrelation Contrast Stretching. *Remote Sensing of Environment*, Vol 42, p 147-155.

Grasty RL. (1976), Applications of gamma radiation in remote sensing. In: *Remote Sensing for Environmental Sciences*, ed. E. Schanda, Springer Verlag, Berlin. p. 257.

Grasty R.L. (1997), Radon emanation and soil moisture effects on airborne gamma-ray measurements. *Geophysics*, vol 62, No 5, pp 1379-1385.

Hey KM. (1999), Desktop assessment and use of on-site indicators as preliminary methods for recognition of acid sulfate soils. *Acid Sulfate Soils & Their Management in Coastal Queensland.* Forum and Technical Papers, Brisbane.

Hsi CD and Langmuir D. (1985), Adsorption of uranyl onto ferric oxyhydroxides: Application of the surface complexation site-binding model. *Geochemica et Cosmochimica Acta* (49), 1931-1941.

Hummel W. (2005), Solubility equilibria and geochemical modelling in the field of radioactive waste disposal. *Pure and Applied Chemistry*, Vol 77, No 3, pp 631-641.

Isbell RF. (1996), *The Australian Soil Classification*. CSIRO Publishing, Melbourne.

Johnston S, Kroon F, Slavich P, Cibilic A and Bruce A, 2003. Restoring the Balance: Guidelines for managing floodgates and drainage systems on coastal floodplains. NSW Agriculture, Wollongbar NSW.

Katz JJ, Seaborg GT and Morss LR. (1986), *Actinide Chemistry*. Chapman and Hall, New York.

Langmuir D. (1978), Uranium solution-mineral equilibria at low temperatures with applications to sedimentary ore deposits. *Geochimica et Cosmochimica Acta*, Vol. 42, pp 547-569.

Langmuir D and Herman JS. (1980), The mobility of thorium in natural waters at low temperatures. *Geochimica et Cosmochimica Acta* 44:1753-1766.

Mitchell JN and Minty BRS. (1998), Clarence Richmond Maclean, Tweed Heads and Eastern Grafton 1:250,000 sheet areas airborne geophysical survey, 1997 – Operations Report. *AGSO Record 1998/27*. Australian Geological Survey Organisation, Canberra.

Morand D (1994), Soil landscapes of the Lismore-Ballina 1:100,000 map sheet. Report, Soil Conservation Service of NSW, Sydney.

Naylor SD. (1997), *Acid Sulphate Soil Risk Map, WARDELL 1:25,000 Sheet*. NSW Department of Land and Water Conservation.

Naylor SD, Chapman GA, Atkinson G, Murphy CL, Tulau MJ, Flewin TC, Milford HB, Morand DT. (1998), *Guidelines for the use of acid sulphate soil risk maps*. Soil Conservation Service of NSW.

Powell B and Ahern CR. (1999), Nature, origin and distribution of acid sulfate soils: Issues for Queensland. *Acid Sulfate Soils & Their Management in Coastal Queensland*. Forum and Technical Papers, Brisbane.

Saksena R.S., Chandra, S, and Singh, B.P. (1974). A gamma transmission method for the determination of moisture content in soils. *Journal of Hydrology*, 23, pp341-352.

Sammut J, White I and Melville MD. (1996) Acidification of an estuarine tributary in Eastern Australia due to drainage of acid sulfate soils. *Marine and Freshwater Research* 47(5).

Smith RJ, Stephenson T, Biffen T and House R. (1995), *Tuckean project, Acid sulfate soil survey*, Unpubl. report.

Troedson A and Hashimoto TR (eds) 2005. NSW coastal quaternary geology data package. NSW Department of Primary Industries, Geological Survey of NSW.

Tulau MJ. (1999a), Acid sulfate soil management priority areas in the lower Richmond floodplain. *Report*, NSW Department of Land and Water Conservation, Sydney.

Tulau MJ. (1999b), Acid sulfate soil management priority areas in the lower Clarence floodplain. *Report*, NSW Department of Land and Water Conservation, Sydney.

White I, Melville MD, Lin C, Sammut J, van Oploo P and Wilson BP. (1995). Fixing problems caused by acid sulphate estuarine soils. *Ecosystem Management: the legacy of science*, ANZAAS '95 Congress.

White I, Melville MB, Wilson BP and Sammut J. (1997) Reducing acidic discharges from coastal wetlands in eastern Australia. In: WJ Streever (ed), *Wetlands Ecology and Management*. 5:55-72. Wetland Rehabilitation Australia.